

Friction of the surface plasmon by high-energy particle-hole pairs: Are memory effects important?

Cesar Seoanez¹, Guillaume Weick^{2;3;4}, Rodolfo A. Jalabert^{2;3}, and Dietmar Weinmann²

¹ Instituto de Ciencia de Materiales de Madrid, CSIC, Cantoblanco E-28049 Madrid, Spain

² Institut de Physique et Chimie des Matériaux de Strasbourg, UMR 7504 (ULP-CNRS), 23 rue du Loess, BP 43, F-67034 Strasbourg Cedex 2, France

³ Institut für Physik, Universität Augsburg, Universitätsstraße 1, D-86135 Augsburg, Germany

⁴ Fachbereich Physik, Freie Universität Berlin, Am Mühlentempel 14, D-14195 Berlin, Germany

April 15, 2024

Abstract. We show that the dynamics of the surface plasmon in metallic nanoparticles damped by its interaction with particle-hole excitations can be modelled by a single degree of freedom coupled to an environment. In this approach, the fast decrease of the dipole matrix elements that couple the plasmon to particle-hole pairs with the energy of the excitation allows a separation of the Hilbert space into low- and high-energy subspaces at a characteristic energy that we estimate. A picture of the spectrum consisting of a collective excitation built from low-energy excitations which interacts with high-energy particle-hole states can be formalised. The high-energy excitations yield an approximate description of a dissipative environment (or "bath") within a finite confined system. Estimates for the relevant timescales establish the Markovian character of the bath dynamics with respect to the surface plasmon evolution for nanoparticles with a radius larger than about 1 nm.

PACS. 73.20.Mf Collective excitations { 78.67.n Optical properties of low-dimensional, mesoscopic, and nanoscale materials and structures { 71.45.Gm Exchange, correlation, dielectric and magnetic response functions, plasmons

1 Introduction

One of the main questions driving the experimental and theoretical research of the last twenty years on metallic nanoparticles is how large in size do we have to go to observe bulk properties. The answer of course depends on the physical property under study. It is furthermore never clearcut. But in many cases the size needed to observe bulk-like behaviour is surprisingly small. Furthermore, the size dependence of quantitative features can already be smooth for very small systems. For instance, the binding energy of Na_9 clusters is quite close to that of Na_8 , even if these two systems are very different from the molecular point of view [1]. Such a continuity points towards the relatively minor importance of the ionic cores and supports the descriptions based on the jellium model, where the conduction electrons are subject to a uniform neutralising background [2]. This view has been validated by the evidence of electronic shells provided by the abundance spectra of alkaline clusters [3]. Within the jellium approximation, the density of electronic states is given by a bulk-like contribution to which we have to add surface and periodic-orbit (or shell) corrections [4].

The optical properties of metallic clusters are dominated by the response of the conduction electrons. Ex-

cept for the smallest clusters, where the transitions between single particle levels dictate the optical response, the optical absorption is dominated by a collective excitation, the surface plasmon. This resonance is located near the classical Mie frequency $\omega_M = \omega_p / \sqrt{3}$, where $\omega_p = (4\pi n_e e^2 / m_e)^{1/2}$ is the bulk plasma frequency and e , m_e , and n_e denote the electronic charge, mass, and density, respectively. Nevertheless, surface effects lead to a reduction of the surface plasmon frequency with respect to the bulk value ω_M [2, 5, 6]. The question of how large the size of the nanoparticle has to be in order to observe a collective excitation in a finite system has the surprising answer that a very small cluster, like for instance Na_6 , may already be enough [7, 8].

For nanoparticle radii a between about 0.5 and 5 nm ($N = 8$ to 14000 conduction electrons for the case of Na) the main effect limiting the lifetime of the resonance is the Landau damping, i.e., decay into particle-hole pairs. The resulting linewidth is given by

$$\gamma_{\text{tot}}(a) = \gamma_i + \gamma_{\text{sc}}(a) + \gamma^{\text{osc}}(a); \quad (1)$$

where γ_i is the intrinsic bulk-like linewidth. The second term in the right-hand side of (1) decreases with the na-

particle size as [9,11]

$$(a) = \frac{3v_F}{4a} g_0 \frac{v_F}{v_M} ; \quad (2)$$

with $v_F = \sqrt{2}k_F^2/2m_e$ and v_F the Fermi energy and velocity, respectively. The monotonically increasing function g_0 is defined as

$$g_0(x) = \frac{1}{12x^2} \frac{np}{x(x+1)} \frac{1}{4x(x+1)+3} \frac{3(2x+1) \ln \frac{p}{x} + \frac{p}{x+1}}{h_p \frac{1}{x(x-1)} \frac{1}{4x(x-1)+3} \frac{3(2x-1) \ln \frac{p}{x} + \frac{p}{x-1}}{1}} \frac{1}{(x-1)^0} ; \quad (3)$$

(x) being the Heaviside step function. The last contribution $\cos(2k_F a) = (k_F a)^{5/2}$ to the linewidth (1) is nonmonotonic in a , and arises from the correlation of the densities of states of the particles and holes [12,13]. It becomes relevant for the smallest sizes of the considered interval, typically for radii in the range 0.5{1.5 nm. For radius larger than 5 nm the Landau damping competes with radiation damping in limiting the lifetime of the resonance. For radius smaller than 0.5 nm the interaction with the ionic background becomes dominant, and the jellium model no longer provides a useful description.

The use of femtosecond pulsed lasers in pump-probe spectroscopy has rendered possible to experimentally address the surface plasmon dynamics [14{17]. The theoretical descriptions built to study this problem [5,6,13,18] treat the collective coordinate as a special degree of freedom, which is coupled to an environment constituted by the degrees of freedom of the relative coordinates. Friction arising from particle-hole pairs has been studied in bulk systems [19]. In the present work we are interested in the case where the excitation spectrum arises from a finite number of particles. The finite number of electrons makes the term "environment" not completely justified in this situation, and leads us to reformulate the above-mentioned question in dynamical terms as: How large in size do we need to go to be allowed to describe the relative coordinates of the electron gas as an environment damping the collective excitation?

This last question is the main subject of the present paper. In particular, we determine which are the energies of the electronic excitations that are active in the damping of the surface plasmon, and which is the characteristic response time of the large enough electronic environment. The latter is important in justifying the Markovian approximation that is assumed to describe the dynamics of the surface plasmon coupled to particle-hole excitations [20].

The paper is organised as follows: In Section 2 we recall the random phase approximation for the surface plasmon and the separation of the excitation spectrum in low- and high-energy particle-hole excitations. In Section 3, we show how the surface plasmon is built from low-energy particle-hole excitations and in Section 4 the cutoff energy

separating the above-mentioned low- and high-energy sectors is determined. In Section 5 the time dynamics of the environment giving rise to the damping of the collective excitation is considered. We end with the conclusions in Section 6.

2 Random phase approximation for the surface plasmon

The understanding of collective excitations in metallic clusters has benefited from the accumulated knowledge in the related problem of nuclear physics, i.e., the description of the giant dipolar resonance [21,22]. The simplest many-body approach yielding collective excitations in a finite system is the Tamm-Dancoff description, where the excited states are built from the Hartree-Fock ground state and all possible one-particle-one-hole (1p-1h) excitations. The basis considered is then mixed by the matrix elements of the residual interaction

$$V_{res} = \frac{1}{4} \sum_{j,i} v_{ji} c_j^\dagger c_i^\dagger c_i c_j V_{HF} ; \quad (4)$$

where c_j^\dagger (c_j) creates (annihilates) the single-particle state j of the Hartree-Fock problem. In the above equation, $v_{ji} = v_{ij}$ with v_{ij} the two-body matrix element of the Coulomb interaction, while

$$V_{HF} = \frac{1}{4} \sum_{j,i} v_{ji} c_j^\dagger c_i c_i^\dagger c_j \quad (5)$$

is the Hartree-Fock interaction Hamiltonian. Diagonalization within this reduced Hilbert space gives the excitation energies. This task is considerably simplified under the assumption that the matrix elements v_{ji} of the residual interaction (4) are separable [23],

$$v_{ji} = d_j d_i ; \quad (6)$$

where $d_j = \langle j | \hat{p} | i \rangle$ are dipole matrix elements and γ is a positive constant characterising the repulsive residual interaction. Within the Tamm-Dancoff approximation, the excitation energies are given by the secular equation

$$\frac{1}{E} = \sum_{ph} \frac{d_{ph}^2}{E_{ph}} ; \quad (7)$$

where p (h) denotes a particle (hole) state above (below) the Fermi level, and $E_{ph} = E_p - E_h$ are particle-hole (p-h) excitation energies.

One important drawback of the Tamm-Dancoff approximation is that its ground state does not include correlations. This is not the case with the random phase approximation (RPA) where the basis of the reduced Hilbert space is built from all possible 1p-1h creations and destructions acting on the ground state. Using again the separability hypothesis (6) for the residual interaction, the RPA secular equation

$$\frac{1}{E} = S(E) \quad (8)$$

is different from (7). Here we have defined the RPA sum

$$S(E) = \sum_{ph} \frac{2}{E^2} \frac{|\mathbf{d}_{ph}|^2}{\epsilon_{ph}^2} : \quad (9)$$

The validity of the RPA [8] and of the separability hypothesis within the time-dependent local density approximation [24] have been well established, even in small clusters.

Nuclear physics textbooks (see, e.g., Ref. [21]) show how to solve the secular equations (7) and (8) graphically under the implicit assumption that the p-h spectrum is bounded in energy. In that case, the solutions of the secular equations are merely renormalizations of the p-h energies ϵ_{ph} except for the largest excitation energy which corresponds to the collective mode. However, it is clear that in a metallic cluster the p-h excitations are not bounded from above on the scale of the plasmon energy. As we will see in the sequel, it is the fast decay of the dipole matrix elements d_{ph} with the p-h energy that ensures the applicability of the standard picture.

An ingenious way of describing the collective excitation in metallic clusters which circumvents the problem of the unbound p-h spectrum is the separation of the reduced 1p-1h RPA Hilbert space in a low-energy sector (the restricted subspace), containing p-h excitations with low energy, and a high-energy sector (the additional subspace) [11,22]. The residual interaction gives rise to the collective excitation as a coherent superposition of a large number of basis states of the restricted subspace. This excitation energy lies in the high-energy sector, and the nonvanishing coupling with p-h states of the additional RPA subspace results in the broadening of the collective resonance. In this approach the cut-off energy separating the two subspaces is somehow arbitrary, as long as it is taken smaller than the resonance energy. The arbitrariness of the cut-off is not problematic for calculating the lifetime of the resonance [11], but the approximate theoretical description of other physical quantities might depend on the cut-off. For example, in the approach where the environment is separated from the low-energy excitations that compose the collective plasmon excitation, the timescales that characterise the dynamics of the electronic environment [20] depend on the cut-off energy. Moreover, it was shown in [6] that the environment-induced redshift of the resonance frequency depends logarithmically on the cut-off. In the following we will provide an estimation of the cut-off energy separating the two subspaces.

3 The surface plasmon as a superposition of low-energy particle-hole excitations

The secular equations (7) and (8) depend crucially on the form of the dipole matrix element d_{ph} . Assuming that the p-h states are confined within a hard-wall sphere, one can decompose [11]

$$d_{ph} = A_{l_p l_h}^{m_p m_h} R_{l_p l_h}(\epsilon_p; \epsilon_h) : \quad (10)$$

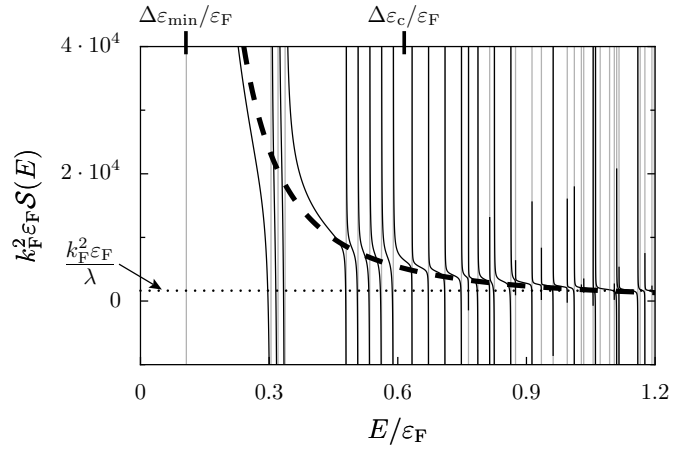


Fig. 1. RPA sum (13) for a Na nanoparticle with $k_F a = 30$ (solid black line). The p-h excitation energies ϵ_{ph} (represented by vertical grey lines) have been obtained from the semiclassical spectrum (41). There are about 15000 degenerate excitations in the interval shown, and the smallest excitation $\epsilon_{min} / \epsilon_F = 10$ has a degeneracy $N = 380$. The dashed line takes only into account the contribution of ϵ_{min} (see Eq. (24)). The cut-off energy ϵ_c separating the two RPA subspaces is also shown in the figure (see Eq. (30)). Above ϵ_c the two sums are close to each other, showing that for high energies the RPA sum is essentially given by the contributions coming from the low-energy p-h excitations. The horizontal dotted line indicates the position of the coupling constant entering the RPA secular equation (8), according to the estimate (25).

The angular part is expressed in terms of Wigner-3j symbols as

$$A_{l_p l_h}^{m_p m_h} = (-1)^{m_p} \frac{q}{(2l_p + 1)(2l_h + 1)} \begin{pmatrix} l_p & l_h & 1 \\ 0 & 0 & 0 \end{pmatrix} \begin{pmatrix} l_p & l_h & 1 \\ m_p & m_h & 0 \end{pmatrix} \quad (11)$$

and sets the selection rules $l_p = l_h \pm 1$ and $m_p = m_h$ for the total and azimuthal angular momenta, respectively. The radial part depends on the energies of the p-h states as

$$R_{l_p l_h}(\epsilon_p; \epsilon_h) = \frac{2\sqrt{2}}{m_e a} \frac{P_{l_p}(\epsilon_p)}{\epsilon_p^2} \frac{P_{l_h}(\epsilon_h)}{\epsilon_h^2} : \quad (12)$$

With the help of equations (10)-(12) and using the appropriate dipole selection rules, we can write the RPA sum (9) as

$$S(E) = \frac{32k_F^2}{3} \frac{\epsilon_F^2}{k_F a} \sum_{\substack{n_h, l_h \\ n_p, l_p = l_h \pm 1}} f_{l_p} \frac{\epsilon_p \epsilon_h}{(E^2 - \epsilon_{ph}^2)^2} \epsilon_{ph}^3 ; \quad (13)$$

where n_h and n_p are radial quantum numbers. We have defined $f_{l_p} = l_h + 1$ if $l_p = l_h + 1$ and $f_{l_p} = l_h$ if $l_p = l_h - 1$. Using the semiclassical quantisations (40) and (41) of Appendix A, we finally obtain the result shown in Figure 1.

In the figure we show (solid black line) the resulting E-dependence of (13). The crossings of this curve with

the horizontal dotted one with height $1 = \gamma$ yield the excitation spectrum within the RPA. The lowest p-h energy estimated in Appendix A is

$$\omega_{m, in} \approx \frac{\omega_F}{k_F a} : \quad (14)$$

Whenever the energy E coincides with a p-h excitation energy ω_{ph} , we have a divergence in $S(E)$ (see vertical grey lines in Fig. 1). For the lowest energies E of the interval considered the sum is dominated by the term associated with the divergence closest to E . On the other hand, for the largest energies E , the fast decay of d_{ph} with ω_{ph} means that the divergences are only relevant for energies extremely close to them. Away from the divergences the sum is dominated by the contributions arising from the low-energy p-h excitations.

To gain physical insight and proceed further in the analysis of the electron dynamics in metallic nanoparticles, we introduce the typical dipole matrix element for states separated by a given energy difference ω ,

$$\begin{aligned} d^{p-h}(\omega) &= \frac{1}{\omega_{p-h}(\omega)} \sum_{\substack{\text{ph} \\ \#_{1=2}}} d_{ph}^2(\omega_{ph}) \\ &= \frac{1}{\omega_{p-h}(\omega)} \sum_{\substack{\text{ph} \\ \#_{1=2}}} d^2 C(\omega; \omega_{ph}) : \quad (15) \end{aligned}$$

Here, we have introduced the local density of dipole matrix elements

$$C(\omega; \omega_{ph}) = \sum_{\text{ph}} d_{ph}^2(\omega_{ph}) \delta(\omega - \omega_{ph}) : \quad (16)$$

As shown in Appendix B, this can be expressed as

$$C(\omega; \omega_{ph}) = \frac{1}{3} \frac{a^2}{\omega^2} F \frac{\omega_{ph}}{\omega} ; \quad (17)$$

where

$$F(x) = (2x+1) \frac{1}{x(x+1)} \ln \frac{x+1}{x} : \quad (18)$$

For $\omega \gg \omega_{ph}$, equation (17) simplifies to

$$C(\omega; \omega_{ph}) \approx \frac{2a^2}{3} \frac{\omega_{ph}^2}{\omega^4} : \quad (19)$$

In expression (15),

$$\omega_{p-h}(\omega) = \sum_{\text{ph}} (\omega_{ph} - \omega)_{+}^{-1} : \quad (20)$$

is the density of p-h excitations with energy ω respecting the dipole selection rules. In order to simplify the presentation, we do not consider spin degeneracy factors. In Appendix C we show that for $\omega \gg \omega_F$ we have

$$\omega_{p-h}(\omega) \approx \frac{(k_F a)^4}{4} \frac{\omega}{\omega_F^2} ; \quad (21)$$

and therefore in such a limit the typical matrix element (15) can be approximated by

$$d^{p-h}(\omega) \approx \frac{2}{3} \frac{a^2}{k_F a} \frac{\omega_F^2}{\omega} : \quad (22)$$

As a check for our estimation of the typical dipole matrix element, we have evaluated the energy-weighted sum rule $\sum_{\text{ph}} \omega_{ph}^2 d_{ph}^2$ using (22) and obtained about 70% of the exact result $(3/4) \sim 2N = 2m_e [2]$. This is quite reasonable regarding all the approximations we made to obtain (22).

In order to illustrate the importance of the low-energy p-h excitations, we present in Figure 1 (dashed line) the contribution to the RPA sum coming only from the infrared p-h excitation energy with the appropriate degeneracy factor N (see Eq. (43) in App. A). Indeed, we can estimate (9) as

$$S(E) \approx N \frac{2 \omega_{m, in} d^{p-h}(\omega_{m, in})^2}{E^2 \omega_{m, in}^2} : \quad (23)$$

With the results (14), (22), and (43), we obtain

$$S(E) \approx \frac{64 k_F^2}{3^5} (k_F a)^3 \frac{\omega_F}{E^2 (\omega_F = k_F a)^2} : \quad (24)$$

While in the lower part of the energy interval in Figure 1 the two curves exhibit considerable discrepancies, in the second half of the interval they are very close (except of course at the divergences). Since the collective excitation is found in this last interval, we see that it is mainly the low-energy p-h excitations that are relevant for the definition of the collective excitation.

Since the resonance energy is known from experiments, we can obtain the value of the coupling constant γ . Indeed, using the estimate (24) evaluated at $E \approx \omega_M$ in the secular equation (8), we obtain

$$\frac{1}{\gamma} \approx \frac{64 k_F^2}{3^5} (k_F a)^3 \frac{\omega_F}{(\omega_M)^2} \quad (25)$$

to leading order in $k_F a \ll 1$. Notice that this result is consistent with the estimate obtained from the energy-weighted sum rule given in [11]. For the case studied in Figure 1, our estimate (25) yields $k_F^2 \omega_F = 1600$. As the radius a increases the lowest p-h energy decreases like $1/a$, the degeneracy at this value increases as a^2 , and the density of p-h excitations contributing to (9), $\omega_{p-h}(\omega)$, grows as a^4 . This increase in the number of excitations contributing to the sum is partially cancelled by the $1/a$ behaviour of the typical dipole matrix element, resulting in a decrease of the coupling constant proportional to the number of particles in the cluster, $1/a^3$, and a value of the plasmon frequency which remains almost unaffected. Therefore, for a larger nanoparticle size, the divergences shown in Figure 1 would be more dense in energy, starting at a lower energy, and the vertical scale would increase as a^3 , thus obtaining a similar value for the plasmon excitation energy ω_M .

4 Separation of the reduced and additional particle-hole subspaces

As we have shown in the last section, the high-energy part of the p-h spectrum is not crucial for the determination of the energy of the collective excitation. In what follows we make this statement more quantitative and estimate the upper-bound cutoff ω_c of the low-energy excitations that we need in order to obtain a stable position of the surface plasmon.

In order to obtain a quantitative estimate of the cutoff, we require that by changing it from ω_c to $(3=2)\omega_c$, the position of the plasmon changes only by a fraction of its linewidth, the smallest energy scale with experimental significance. Our criterion leads to the condition

$$S_{\omega_c}(\omega_M) = S_{\frac{3}{2}\omega_c}(\omega_M + \gamma); \quad (26)$$

with the RPA sum S that has been defined in (9). The additional subscript refers to the upper bound of the p-h energies.

The left-hand side of (26) can be estimated according to

$$S_{\omega_c}(\omega_M) \approx \sum_{\omega_{min}}^{\omega_c} d\omega^{p-h}(\omega) \frac{2\omega^{d^{p-h}(\omega)^2}}{(\omega_M)^2 \omega^2}; \quad (27)$$

with d^{p-h} and ω^{p-h} as defined in (15) and (20), respectively. Using (21) and (22), we obtain

$$S_{\omega_c}(\omega_M) \approx \frac{4k_F^2}{3^2} k_F a \frac{\omega_F^2}{\omega_M} \frac{1}{\omega_{min}} \frac{1}{\omega_c} \quad (28)$$

to leading order in $k_F a$. Similarly,

$$S_{\frac{3}{2}\omega_c}(\omega_M + \gamma) \approx \frac{4k_F^2}{3^2} k_F a \frac{\omega_F^2}{\omega_M} \left(1 + \frac{2}{\omega_M} \frac{1}{\omega_{min}} \frac{2}{3\omega_c} \right); \quad (29)$$

Using the expressions (2) and (14) for ω_{min} and ω_M , respectively, finally yields according to the criterion (26) the cutoff energy

$$\omega_c \approx \frac{\omega_F}{9g_0(\omega_F/\omega_M)} \omega_M; \quad (30)$$

with the function g_0 defined in (3). For Na clusters, we have $\omega_F/\omega_M = 0.93$ and our criterion yields a value $\omega_c \approx (3=5)\omega_F$.

We have verified the robustness of our criterion (26) by exploring different physical parameters, like the size of the cluster. Indeed, it can be seen in Figure 1 that above ω_c the RPA sum evaluated from (13) (solid line) and the estimate (24) (dashed line) are close to each other, showing that for high energies the RPA sum is essentially given by the contributions coming from the low-energy p-h excitations. We have checked that this feature of ω_c is independent of the size a of the nanoparticle.

In order to have a well-defined collective excitation, the cutoff energy ω_c must obviously be larger than the minimum p-h excitation energy (14). For Na, we find that this condition is already verified with only $N = 20$ conduction electrons in the nanoparticle, in agreement with the experiments of reference [7] and the numerical calculations of reference [8].

The splitting in low and high-energy p-h excitations is important in order to justify the separation of the electronic degrees of freedom into centre-of-mass and relative coordinates [5, 6, 13, 18]. Within such an approach, the Hamiltonian of the electronic system is written as

$$H = H_{cm} + H_{rel} + H_c; \quad (31)$$

The first term describes the centre-of-mass motion as a harmonic oscillator. The second term describes the relative coordinates as independent fermions in the effective mean-field potential. The coupling term H_c describes the creation or annihilation of a surface plasmon by destruction or creation of p-h pairs. Its strength is given by the coupling constant $\lambda = (\omega_e/\omega_M)^3 = 2N$ and the dipole matrix element d_{ph} [6]. It is important to remark that, even if we have used the separability hypothesis of the residual interaction to justify the decomposition (31), the model that is put forward does not rely on such an approximation.

5 Dynamics of the relative-coordinate system

The decomposition (31) of H suggests to treat the collective coordinate as a simple system of one degree of freedom which is coupled to an environment with many degrees of freedom. The latter are the relative coordinates described by H_{rel} . This is the approach taken in [20]. In this picture, the time evolution of the centre-of-mass system (i.e., the surface plasmon) strongly depends on the dynamics of the relative-coordinate system. Such a dynamics is characterised by a correlation function which can be written at zero temperature as [20]

$$C(t) = \sum_{ph}^X d_{ph}^2 \int e^{i\omega_{ph}t} (\omega_{ph} - \omega_c); \quad (32)$$

In order to evaluate the above expression, it is helpful to introduce its Fourier transform

$$(\omega) = \sum_{ph}^X d_{ph}^2 (\omega - \omega_{ph}) (\omega_{ph} - \omega_c) \quad (33)$$

which has been calculated in [6]. Finite temperatures were shown to result in a small quadratic correction. Consistently with the results of the preceding sections, we employ our low energy estimates (21) and (22) to obtain

$$(\omega) \approx \frac{3v_F}{4a} \frac{\omega_M^3}{\omega} (\omega - \omega_c); \quad (34)$$

This result is consistent with the one of reference [6] (see Eq. (34) in there) in the limit $\omega \sim \omega_M$ and for zero temperature.

In principle we could calculate $C(t)$ by taking the inverse Fourier transform of (34). The decay of $C(t)$ for very long times is dominated by the discontinuity of ϵ'' at ω_c . This is somehow problematic since ω_c can only be estimated as we did in Section 4, and since the functional form of the long time decay depends on how sharply the cutoff is implemented. However, it is important to realise that it is not the very long time behaviour that determines the relevant decay of the correlation function, but rather the typical values at which $C(t)$ is reduced by an important factor from its initial value $C(0)$. We then estimate the correlation time as the mean decay time of $C(t)$,

$$h_{\text{cor}} = \frac{\int_0^\infty dt t \frac{d}{dt} \frac{C(t)}{C(0)}}{\int_0^\infty dt C(t)} : \quad (35)$$

If $C(t)$ were an exponentially decreasing function, h_{cor} would simply reduce to the inverse of the decay rate. Using the definition (33), we get

$$h_{\text{cor}} = \frac{\int_0^\infty dt \epsilon''(\omega)}{\int_0^\infty dt \epsilon''(\omega_c)} : \quad (36)$$

Given the fast decay of the function $\epsilon'' = \omega_c^{-3}$, the above integrals are dominated by their lower limit ω_c and we have

$$h_{\text{cor}} \sim \frac{2}{3} \frac{1}{\omega_c} : \quad (37)$$

Since ω_c is of the order of $(3-5)\epsilon_F$, we see that the response time (or correlation time) of the electronic environment is of the order of its inverse Fermi energy.

The estimation of the characteristic response time of the electronic environment is crucial in justifying the Markovian approximation used in [20]. In that work, the degrees of freedom corresponding to the relative coordinates were integrated out and treated as an incoherent heat bath that acts on the collective coordinate. Such an approach relies on the fast response of the environment as compared to the time evolution of the surface plasmon. The typical scale for the latter is the inverse of the decay rate, $\tau_{\text{sp}} = 1/\gamma$. Using (2) and (30), we therefore have

$$\frac{\tau_{\text{sp}}}{h_{\text{cor}}} = \frac{9 \epsilon_0 (\epsilon_F \sim \omega_c)^2}{\omega_c^3} k_F a : \quad (38)$$

For the example of Na nanoparticles worked in Section 3, we have $\tau_{\text{sp}} = h_{\text{cor}} / k_F a$. This is a safe limit since in not too small nanoparticles, $k_F a \gg 1$. As the size of the cluster increases, the applicability of the Markovian approximation is more justified. This is expected since the electronic bath has more and more degrees of freedom, approaching an "environment" in the sense of quantum dissipation. Since the physical parameters of alkaline nanoparticles entering (38) are close to that of noble-metal clusters, the dynamics of the surface plasmon can be expected to be Markovian in that case too.

6 Conclusions

We have studied the role of particle-hole excitations on the dynamics of the surface plasmon. A key concept in this analysis is the separation into low-energy excitations which lead to the collective excitation once they are mixed by the residual interaction, and high-energy excitations that act as an environment damping the resonance. Using the random phase approximation and assuming the separability of the residual interaction, we have established a criterion for estimating the cutoff energy separating the low- and high-energy subspaces. The resulting cutoff energy is approximately $(3-5)\epsilon_F$ for the case of Na nanoparticles.

Since the number of electrons in the cluster is finite, the assumption that the high-energy particle-hole excitations act on the collective excitation as an environment, introducing friction in its dynamics, may be questionable. What settles this issue is the ratio between the typical evolution time of the collective excitation and the one of the high-energy particle-hole excitations. The former is given by the inverse of the plasmon linewidth, while the latter is obtained from the decay of the correlation function of the environment. We have found that this ratio improves with increasing cluster size. Even for a small cluster with $a = 1 \text{ nm}$, the ratio is approximately 10, justifying the use of the Markovian approximation which assumes a fast time evolution of the environment with respect to the one of the collective excitation.

The relevance of memory effects in the electronic dynamics of small clusters is of current interest, due to the advance in time-resolved experimental techniques [14,17]. First-principle calculations have recently addressed this issue by comparing time-dependent density functional theories with and without memory effects for small gold clusters [25]. For very small clusters ($N < 8$) memory effects were shown to be important. We stress that the memory considered in [25] is that of the electron gas as a whole, while we are concerned in this work with the memory arising from the dynamical evolution of the relative-coordinate subsystem. It would be interesting to consider cluster sizes intermediate between the ones considered in the present work and those of reference [25] in order to study the emergence of memory effects.

We thank F. Guinea, G.-L. Ingold, and E. Mariani for helpful discussions. We acknowledge financial support from the ANR, the Deutsche Forschungsgemeinschaft, the EU through the MCRTN program, the French-German PAI program Procope, and the Ministerio de Educacion y Ciencia (MEC).

A Lowest energy of the particle-hole spectrum

If we consider the cluster as a hard-wall sphere of radius a , its eigenstates are given in terms of spherical Bessel functions. Using the large ka expansion of the latter (see clas-

sical high-energy limit), the quantisation condition reads

$$ka = \frac{1}{2} + n \quad (39)$$

with l and n non-negative integers. The energy of a single-particle (hole) state is related to its wavevector $k_{p(h)}$, its total angular momentum $l_{p(h)}$, and its radial quantum number $n_{p(h)}$ as

$$\begin{aligned} \epsilon_{p(h)} &= \frac{\hbar^2 k_{p(h)}^2}{2m_e} \\ &= \epsilon_F \frac{1}{k_F a} \left(\frac{l_{p(h)}}{2} + n_{p(h)} \right)^2 : \end{aligned} \quad (40)$$

Thus, the energy of a p-h excitation entering the RPA sum (13) is

$$\begin{aligned} \epsilon_{ph} &= \epsilon_F \frac{1}{k_F a} \left(\frac{l_p}{2} + n_p \right) + \epsilon_F \frac{1}{k_F a} \left(\frac{l_h}{2} + n_h \right) \\ &= \epsilon_F \frac{1}{k_F a} \left(\frac{l_p + l_h}{2} + n_p + n_h \right) : \end{aligned} \quad (41)$$

Notice that using the exact quantum mechanical spectrum in (13) would not change significantly the result depicted in Figure 1, since the approximation (39) is very reliable for states close to the Fermi energy. We have also checked that generating the p-h excitation energies randomly in the RPA sum (9) does not affect the physical picture of Figure 1. Indeed, the main ingredient to understand such a picture is the fast decay of the dipole matrix element with the p-h energy.

The expressions for the dipole matrix element (12) as well as for the typical dipole matrix element (22) diverge in the limit of a small p-h energy. It is therefore crucial for our analysis to determine the appropriate minimum energy ϵ_{min} that renders this divergence unphysical.

This can be achieved by imposing the dipole selection rules in (41) and that the energy difference is minimal. The first condition dictates that $l_h = l_p - 1$ and $m_h = m_p$. Therefore there are two ways of obtaining the minimal energy difference: $n_p = n_h$ with $l_p = l_h + 1$ and $n_p = n_h + 1$ with $l_p = l_h - 1$. In both cases we have

$$\epsilon_{min} \sim \frac{\epsilon_F}{k_F a} \frac{k_h}{k_F} : \quad (42)$$

Since we are interested in states close to the Fermi level, we can simplify (42) to expression (14).

If we consider sodium clusters with $k_F a = 30$ ($a = 3.3$ nm and $N \sim 4000$ conduction electrons per spin direction), we have $\epsilon_{min} \sim \epsilon_F/10$. This is a much larger energy than the lowest one we can observe in the numerically generated excitation spectrum (see Fig. 1 in Ref. [12]). However, the two results are reconciled once we take into account the large degeneracy yielded by our approximate quantisation condition (39).

The degeneracy of p-h excitations with minimal energy is given by twice the number of pairs (l_h, n_h) compatible

with $k_h = k_F$ and $\epsilon_{ph} = \epsilon_{min}$. Indeed, we have seen that there are two possible particle states p starting from h and verifying the above-mentioned conditions. For each n between 1 and $k_F a$, there is a value of $l = 2(k_F a - n)$ and therefore the number of degenerate p-h excitations with energy ϵ_{min} is

$$\begin{aligned} N &= 2 \sum_{n=0}^{k_F a} (2l + 1) \\ &= 2 \sum_{n=0}^{k_F a} 4 \frac{k_F a}{2} (n + 1) \\ &= 4 \frac{k_F a}{2} : \end{aligned} \quad (43)$$

This degeneracy factor has to be included in Figure 1, and it is crucial for the determination of the collective excitation.

B Local density of the dipole matrix element

Equation (16) defines the local density of dipole matrix elements connecting states at energies ϵ and $\epsilon + \epsilon'$. We used particle and hole states in our definition, since this is the main interest of our work. But note that the calculation presented in this appendix is not restricted to that case and can be easily extended to any states. The result would be of course unchanged.

Local densities of matrix elements of arbitrary operators have been thoroughly studied as they can be easily connected with physical properties, ranging from far-infrared absorption in small particles [26] to electronic lifetimes of quantum dots [27]. A semiclassical theory for the local density of matrix elements has been developed [28-30], where (16) can be expressed as a smooth part given by correlations along classical trajectories plus a periodic orbit expansion. We will not follow here this general procedure, but use the simple form of the dipole matrix elements (10) for states confined in a hard-wall sphere and the semiclassical approximation applied to the radial (fixed l) problem [12,13].

Introducing the local density of states, which in leading order in ϵ is given by

$$\rho_1(\epsilon) = \frac{1}{2\pi} \frac{d}{d\epsilon} \left(\frac{2m_e a^2 \epsilon}{\hbar^2} \right)^{1/2} (1 + 1/2\epsilon^2) ; \quad (44)$$

we can write with the help of equations (10)-(12)

$$\begin{aligned} C(\epsilon; \epsilon') &= \frac{2\pi^2}{m_e a} \sum_{l_{max}} \frac{\epsilon'^{l_{max}}}{3\epsilon'^4} \\ &\quad \sum_{l_h=0}^{l_{max}} \rho_{l_h}(\epsilon') [(l_h + 1)\rho_{l_h+1}(\epsilon'^0) + l_h \rho_{l_h-1}(\epsilon'^0)] \end{aligned} \quad (45)$$

where l_{max} is the maximum allowed l_h for an energy ϵ' , while $\epsilon'^0 = \epsilon + \epsilon'$. In the semiclassical limit we can take

